J. Membrane Biol. 201, 139–155 (2004)
DOI: 10.1007/s00232-004-0712-9

The Journal of
Membrane
Biology

Time-dependent Interactions of Glibenclamide with CFTR: Kinetically Complex Block of Macroscopic Currents

Z.-R. Zhang[1], G. Cui[1], S. Zeltwanger[2], N.A. McCarty[1]
[1]School of Biology, Georgia Institute of Technology, Atlanta, GA 30332-0230, USA
[2]Department of Physiology, Emory University School of Medicine, Atlanta, GA 30322, USA

Received: 15 June 2004/Revised: 16 August 2004

Abstract. Blockade of the CFTR chloride channel by glibenclamide was studied in *Xenopus* oocytes using two-electrode voltage-clamp recordings, macropatch recordings, and summations of single-channel currents, in order to test a kinetic model recently developed by us from single-channel experiments. Both the forward and reverse macroscopic reactions, at negative and positive membrane potential V_M, respectively, were slow in comparison to those reactions for other CFTR pore blockers such as DPC and NPPB, resulting in prominent relaxations on the order of tens of milliseconds. The rate of the reverse reaction was voltage-dependent, and dependent on the Cl^- driving force, while that of the forward reaction was not. In inside-out macropatches, block and relief from block occurred in two distinct phases that differed in apparent affinity. The results are consistent with the presence of multiple glibenclamide binding sites in CFTR, with varying affinity and voltage dependence; they support the kinetic model and suggest experimental approaches for identification of those sites by mutagenesis.

Key words: Cystic fibrosis transmembrane conductance regulator — Chloride Channel — Blocker — ABC Transporter — Sulfonylurea

Introduction

The gene defective in cystic fibrosis encodes the cystic fibrosis transmembrane conductance regulator (CFTR), a large integral membrane protein found in the plasma membranes of many epithelial cells (Riordan et al., 1989). The predicted secondary structure of CFTR places it in the superfamily of ATP-binding cassette (ABC) transporters or traffic ATPases (Higgins & Linton 2003). CFTR has multiple roles in epithelial cells: it forms a low-conductance chloride channel, which participates in transepithelial chloride movement, and it also regulates other ion channels in these same membranes (Al-Awqati, 1995). Several pharmacological agents have been shown to inhibit CFTR Cl^- currents through pore blockade (*reviewed in* McCarty, 2000; Dawson et al., 2003). These include members of the arylaminobenzoates such as diphenylamine-2-carboxylate (DPC), flufenamic acid (FFA), and 5-nitro-2-(3-phenylpropylamino)-benzoate (NPPB) (McCarty et al., 1993; Walsh, Long & Shen, 1999; Zhang, Zeltwanger & McCarty, 2000a), and members of the sulfonylureas (Schultz et al., 1996; Sheppard & Robinson, 1997). Pore-blocking drugs maybe used as probes in efforts to determine structural features of the pore. For use in this way, it is helpful if the drugs interact with the channel in a straightforward manner, indicative of a single class of drug-channel interactions.

Our previous studies of the microscopic kinetics of block of single WT-CFTR channels by glibenclamide under steady-state conditions described multiple classes of interactions between drug and channel that differed in concentration-, voltage-, and pH-dependence, which may reflect interactions with different sites (Zhang, Zeltwanger & McCarty, 2004). Some interactions were characterized by rapid kinetics, some intermediate, and some slow, representing transitions between the open state and three glibenclamide-induced blocked states that we termed C1, C2, and C3, respectively (Fig. 1). State C1 is characterized by the fastest forward and reverse rates, while state C3 is characterized by the slowest forward and reverse rates. The kinetics of glibenclamide's interactions with the fast and intermediate

Correspondence to: N.A. McCarty; email: nael.mccarty@biology.gatech.edu

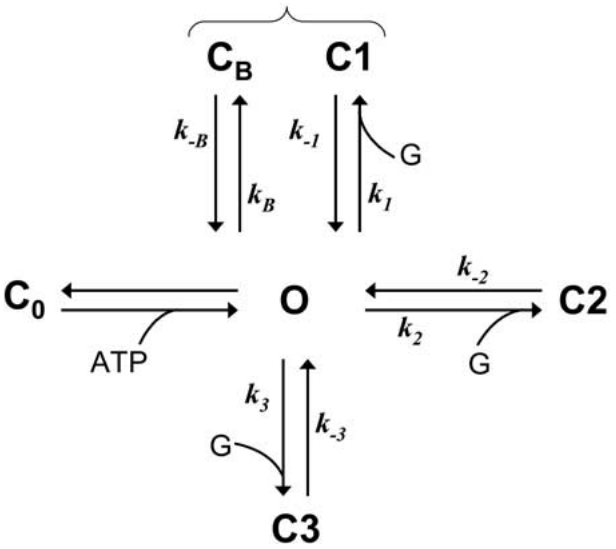

Fig. 1. Kinetic model for block of WT-CFTR channels by glibenclamide, derived from single-channel recordings (Zhang et al., 2004). Phosphorylated channels open in an ATP-dependent manner from state C_0 to state O. From there, channels may be blocked with rapid kinetics by the background blocker, leading to the C_B state, or by interactions with glibenclamide (G), leading to the C1 state. The C_B and C1 states are kinetically indistinguishable at a given glibenclamide concentration, as they are both characterized by blocked states < 1 ms in duration. Glibenclamide also interacts with two other sites with intermediate and slow kinetics leading to the C2 and C3 states, respectively. Rate constants discussed in the text are shown in italics.

kinetic states (C1 and C2) are on the same order as the kinetics of interaction with DPC and NPPB, two arylaminobenzoates, which have been used as probes of the CFTR pore due to their voltage-dependent blockade (McCarty et al., 1993; McDonough et al., 1994; Zhang et al., 2000a). Block of CFTR macroscopic currents by DPC or NPPB is time-independent, reflecting rapid interactions with a single class of drug-binding sites (Zhang et al., 2000a). However, the disparate kinetics of interaction between glibenclamide and its multiple apparent binding sites predict that block of macroscopic currents by this drug may be complex: the slow kinetics of glibenclamide's interaction with the C3 state suggest that block of CFTR whole-cell and macroscopic currents by this drug should exhibit time dependence.

The present study was undertaken to test several predictions arising from our kinetic description of block of CFTR single channels by glibenclamide (Zhang et al., 2004). First, we compare the kinetics of whole-cell currents measured using the two-electrode voltage-clamp technique (TEVC currents) from oocytes expressing wildtype (WT)-CFTR in the presence of DPC or NPPB, as simple pore blockers, with the kinetics of such currents in the presence of glibenclamide. Secondly, we show that such kinetic studies are greatly facilitated by using the excised, inside-out macropatch configuration, which eliminates several difficulties associated with analysis of TEVC currents. We then asked whether the voltage dependence and concentration dependence of the kinetics of blockade of macroscopic currents were consistent with the microscopic kinetics of interaction with each site identified in single-channel experiments. The results confirm the kinetic model derived from single-channel studies in WT-CFTR and suggest new quantitative approaches for determining the effects of site-directed mutations at the (presumably separate) glibenclamide-binding sites in the channel pore.

Materials and Methods

Preparation of Oocytes and cRNA Injection

Most of the methods used are similar to those described previously (McCarty et al., 1993; McDonough et al., 1994). Briefly, stage V–VI oocytes from *Xenopus* were prepared as described (Quick et al., 1992) and were incubated at 18°C in a modified Liebovitz's L-15 medium with addition of HEPES (pH 7.5), gentamicin, penicillin, and streptomycin. cRNA was prepared from a construct carrying the full coding region of CFTR in the pAlter vector (Promega; Madison, WI; *see* McDonough et al., 1994). For measurement of TEVC currents and for single-channel recordings, oocytes were injected with 5 to 19 ng of CFTR cRNA plus 0.6 ng of cRNA for the human β_2-adrenergic receptor (β2-AR), which allows activation of PKA-regulated currents by addition of isoproterenol (ISO) to the bath. For macropatch recordings, oocytes were injected with 30–100 ng of cRNA for CFTR only. Recordings were made at room temperature, 48–96 hours after injection.

Electrophysiology

TEVC Currents

Standard two-electrode voltage-clamp techniques were used to study whole-cell macroscopic currents. Electrodes were pulled from borosilicate glass (Sutter Instrument Co.; Novato, CA) and filled with 3 M KCl. Pipette resistances measured 0.4 – 0.9 MΩ in bath solution. Two-electrode voltage-clamp data were acquired using a GeneClamp 500 amplifier and pCLAMP software (version 8.0 or 8.2; Axon Instruments, Union City, CA); currents were filtered at 500 Hz. Normal bath solution for whole-cell experiments (ND96) contained (in mM): 96 NaCl, 2 KCl, 1 $MgCl_2$, and 5 HEPES. For different experiments, the pH of the bath solution was adjusted to 6.5 or 7.5 with NaOH. The low Cl^- bath solution contained 90 mM Na-isethionate in place of 90 mM NaCl. Oocytes were activated by superfusion of ND96 containing ISO at 0.1–5 μM final concentration. For calculation of voltage dependence and macroscopic kinetics of block, the membrane potential (V_M) was stepped for 75 ms from the holding potential (−30 mV) to a range of potentials from –140 mV to +80 mV, at 20 mV increments. This voltage protocol was chosen for these experiments in order to limit activation of background conductances and to allow comparison of block by glibenclamide to block by DPC and NPPB studied under the same conditions (McCarty et al., 1993; Zhang et al., 2000a). Oocytes were first activated in the absence of blocker by incubation with ISO for 6 – 7 minutes, until currents peaked. The bath solution was then exchanged for one containing 100 μM

glibenclamide without ISO. Oocytes were incubated in this solution for 20 minutes, in order to load drug into the cell, and were then activated again by ISO in the continuing presence of glibenclamide. In some experiments, bath pH was reduced to 6.5 in order to enhance loading of the drug from bath into cytoplasm (the pKa of glibenclamide was reported to be 6.3 (Sheppard & Robinson, 1997); *see* Zhang et al., 2000a). For experiments with DPC or NPPB, these drugs were added to ND96 + ISO and allowed to reach steady-state inhibition of CFTR over the course of ~7 minutes (Zhang et al., 2000a). For experiments including NPPB, all solutions contained 1 mM Ba^{2+} to limit activation of endogenous Cl^- channels.

Analysis. Macroscopic currents from TEVC experiments were analyzed using the Clampfit program of pCLAMP. Background currents at each potential before exposure to ISO and after washout were subtracted to determine the cAMP-dependent current. For analysis of the voltage dependence of macroscopic block, data were separately analyzed over two time periods: the first 2 ms following the voltage step (early phase currents), and the last 10 ms (late phase currents) of each 75 ms episode. To determine voltage dependence of block, affinity at each potential and during each phase was expressed as the apparent K_D, and was calculated as:

$$\text{Apparent } K_D\,(V) = [drug]_{\text{bath}} \bullet \frac{I}{I_0 - I} \qquad (1)$$

where for each voltage V, I_0 is the current level in the absence of blocker and I is the current level in the presence of drug. In this context, it is important to point out that we do not know the actual concentration of drugs in the cytoplasm during whole-cell experiments.

Kinetics of block of TEVC currents by glibenclamide were estimated by fitting second-order exponential functions to the background-subtracted current records. Under many conditions, the 75 ms duration of the voltage pulse used for TEVC experiments was not long enough to reach true steady state; hence, the values presented as kinetics of blockade must be considered estimates at best and for the forward reaction most likely are underestimates. Time constants for relaxations of macroscopic currents from whole-cell experiments will be described by the upper-case tau (T).

Macropatch Experiments

All macropatch studies were performed on excised, inside-out patches. Oocytes were shrunk in a hypertonic solution (in mM: 200 monopotassium aspartate, 20 KCl, 1 $MgCl_2$, 10 EGTA, and 10 HEPES-KOH, pH 7.2) and the oocyte vitelline membrane was then removed. Pipettes were pulled from borosilicate glass (Sutter), and had an average resistance of ~1 MΩ when filled with pipette solution (in mM: 150 NMDG-Cl, 5 $MgCl_2$, and 10 TES, adjusted with Tris to pH 7.4). Seal resistances were in the range of >200 GΩ. After excision, the chamber was perfused with intracellular solution (150 NMDG-Cl, 1.1 $MgCl_2$, 2 Tris-EGTA, 1 MgATP, 10 TES, pH adjusted to 7.3 with Tris). Application of 50 U/mL PKA (Promega) was used to activate CFTR. Channel currents were recorded at room temperature (~22°C) with an Axopatch 200B amplifier (Axon) and filtered with a 4-pole Bessel filter (Warner Instruments; Hamden, CT) at 0.1 kHz before being acquired by the computer at 100 μs / point using the Clampex program of pCLAMP 8.2 (Axon).

Data were analyzed using Clampfit 8.2 or 9.0 (Axon). Solutions were exchanged rapidly using a fast-perfusion system (Warner Instruments) controlled by pCLAMP software; the resolution of this system was ~25 ms as judged by activation of endogenous calcium-activated chloride channels (*data not shown*). Rapid solution exchange in macropatch experiments limits concerns about channel rundown between control and experimental recordings. Time-constants for relaxations of macroscopic currents from macropatch experiments will be described by the lower-case tau (τ).

Single-Channel Studies

Oocytes were prepared for study in the same way as for macropatch experiments. After excision into the inside-out configuration, the chamber was perfused with intracellular solution containing 1 mM MgATP and channels were activated by PKA. CFTR currents were recorded at room temperature (~22°C) with an AI2120 amplifier (Axon) at 10 kHz to DAT tape. Data were subsequently played back and filtered with a 4-pole Bessel filter (Warner) at 1 kHz and acquired by the computer at 100 μs / point using the Fetchex program of pCLAMP 8.2 (Axon).

Single-Channel Summations. Relaxations of summations of single acetylcholine-receptor channels were used previously to differentiate the effects of ion-channel blocking drugs (intraburst closures) from termination of channel bursts after nearly synchronous opening due to quantal release of acetylcholine (Neher & Steinbach, 1978; *see also* Colquhoun & Hawkes, 1995). This analysis of current relaxations enabled distinction between inhibitory effects (states) that exhibit markedly different frequencies of occurrence, and therefore, markedly different on-rates. In the acetylcholine receptor study, summations distinguished between fast pore-block and slower channel closure by gating. In the present study, we used this strategy not to separate channel blocking effects from cessation of a CFTR open burst, but rather to differentiate between fast and slow intraburst blocking effects, given that the microscopic rates to these states differ significantly (Zhang et al., 2004).

Well-separated bursts were studied in patches with low channel activity. The first 200 ms of 82 – 153 bursts, in each condition, were aligned with respect to the initiation of the burst, and were summed. We chose a cutoff of 200 ms in order to avoid contaminating the effects of slow blockade with the termination of a burst, which would complicate the interpretation of this analysis by decay caused by gating closures as opposed to decay caused by intraburst blockade. The fact that no slow component of current decay is observed in the absence of blocker (*see* Fig. 9), strongly implies that this analysis was not contaminated by gating closures and confirms that the slow portion of the biphasic decay in single-channel summations is due to blockade by glibenclamide.

Statistics

Unless otherwise noted, values given are mean ± SE. Statistical analysis was performed using the t-test for paired or unpaired measurements (SigmaStat, Jandel Scientific; San Rafael, CA), as appropriate for each set of experiments, with $P \leq 0.005$ or $P \leq 0.05$ considered indicative of significance.

Source of Reagents

Unless otherwise noted, all reagents were obtained from Sigma Chemical (St. Louis, MO). DPC (*N*-phenylanthranilic acid) was from Aldrich Chemical (Milwaukee, WI); NPPB (5-nitro-2-(3-phenylpropylamino)benzoic acid was from RBI (Natick, MA); L-15 medium was from Gibco/BRL (Gaithersburg, MD). Glibenclamide, DPC, and NPPB were prepared as stock solutions in DMSO at 0.1 M. At the dilutions used, DMSO was without effect on CFTR currents (*not shown*).

Results

Slow, Time-dependent Inhibition

Glibenclamide, DPC, and NPPB are voltage-dependent blockers, each accessing their binding sites from the cytoplasmic end of the pore. Figure 2 shows ISO-activated TEVC currents in an oocyte expressing the β_2-adrenergic receptor and WT-CFTR in the absence of drug and after twenty minutes of incubation in the presence of 100 μM glibenclamide. Whole-cell CFTR currents in the presence of glibenclamide exhibited time-dependent block at hyperpolarizing potentials and time-dependent relief from block at depolarizing potentials. Such time-dependent behavior may reflect interactions between the drug and separate binding sites that differ kinetically. To test the predictions of the multistate model derived from single-channel studies (Zhang et al., 2004), we have characterized block of CFTR macroscopic currents using three approaches: block of TEVC macroscopic currents, block of currents in excised, inside-out macropatches, and summations of currents from excised, inside-out single-channel patches.

Kinetics of Block at Hyperpolarizing Potentials

TEVC Currents

In the absence of added blocker, whole-cell CFTR currents at hyperpolarizing potentials in TEVC experiments exhibited a brief relaxation (Fig. 3 *left*) that is due to block of the pore by an unknown cytosolic component (Hanrahan & Tabcharani, 1990; Haws et al., 1992; McCarty et al., 1993; Winter et al., 1994; Ishihara and Welsh, 1997; Mathews et al., 1998; Zhang et al., 2004); hereafter, we will refer to this phenomenon as "background block" (C_B in Fig. 1). As described previously (McDonough et al., 1994; Zhang et al., 2000a) currents measured in the presence of 100 μM DPC or 100 μM NPPB continued to exhibit the brief relaxation due to background block, but the peak inward currents and currents at steady state were inhibited further compared to currents in the absence of blocker (Fig. 3*B*, 3*C*). Most importantly, DPC and NPPB do not themselves induce significant time dependence in the TEVC currents, which is consistent with the rapid forward microscopic rates for block by these drugs.

In contrast, TEVC currents from oocytes incubated in the presence of 100 μM glibenclamide exhibited the following three components (Fig. 3*D* *left*). First, the peak currents observed upon stepping to hyperpolarizing potentials were inhibited by 14.0 ± 2.3 % (at V_M = −100 mV and pH = 7.5; n = 8). If this phenomenon is due to glibenclamide, the magnitude of inhibition of peak currents should be concentration-dependent. To test this, we made

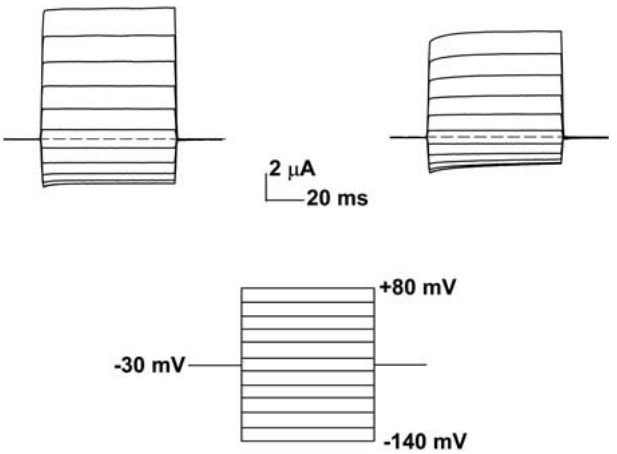

Fig. 2. Voltage-dependent block of CFTR TEVC currents by glibenclamide. Families of currents in the absence of drug (*control, left*) and in the presence of 100 μM glibenclamide (*right*) for WT-CFTR, using the voltage protocol shown below. Dashed lines indicate position of zero current. The voltage protocol is shown at bottom.

use of the greater extent of block achieved when the oocytes were incubated with glibenclamide at bath pH 6.5 (*see* Methods). At this reduced pH, peak currents were inhibited by 5.4 ± 1.0% and 53.8 ± 1.3 % at bath glibenclamide concentrations of 25 μM and 100 μM, respectively (n = 4 – 5; P < 0.001). This fast, time-independent inhibition likely reflects interactions of glibenclamide with the sites corresponding to the C1 and C2 states (k_1 and k_2 in Fig. 1) which occur with kinetics very similar to that for block by DPC and NPPB, which also do not produce time-dependent behavior. The decrease in peak currents may also reflect a small degree of rundown of CFTR currents during the time required for the drug to cross the plasma membrane.

The second component shown in Fig. 3*D* (*left*), in the presence of glibenclamide, is a current relaxation that is fit best with a second-order exponential, reflecting contributions from two separate processes. The time constant describing the faster component ($T_{ON,1}$) very closely matches the time constant for background block seen in the absence of glibenclamide (Table 1). Furthermore, there was no relationship between glibenclamide concentration and the magnitude of the decrease in current due to the faster time-dependent component (which usually comprises less than 20% of the observed time-dependent inhibition). Hence, this component of the relaxation is not due to a glibenclamide-induced event, and simply represents the continuing presence of background block in whole-cell records in the presence of glibenclamide.

The major component of the time-dependent inhibition of TEVC currents ($T_{ON,2}$) arises from slowly-developing block by glibenclamide that approaches steady-state; the voltage pulse in these

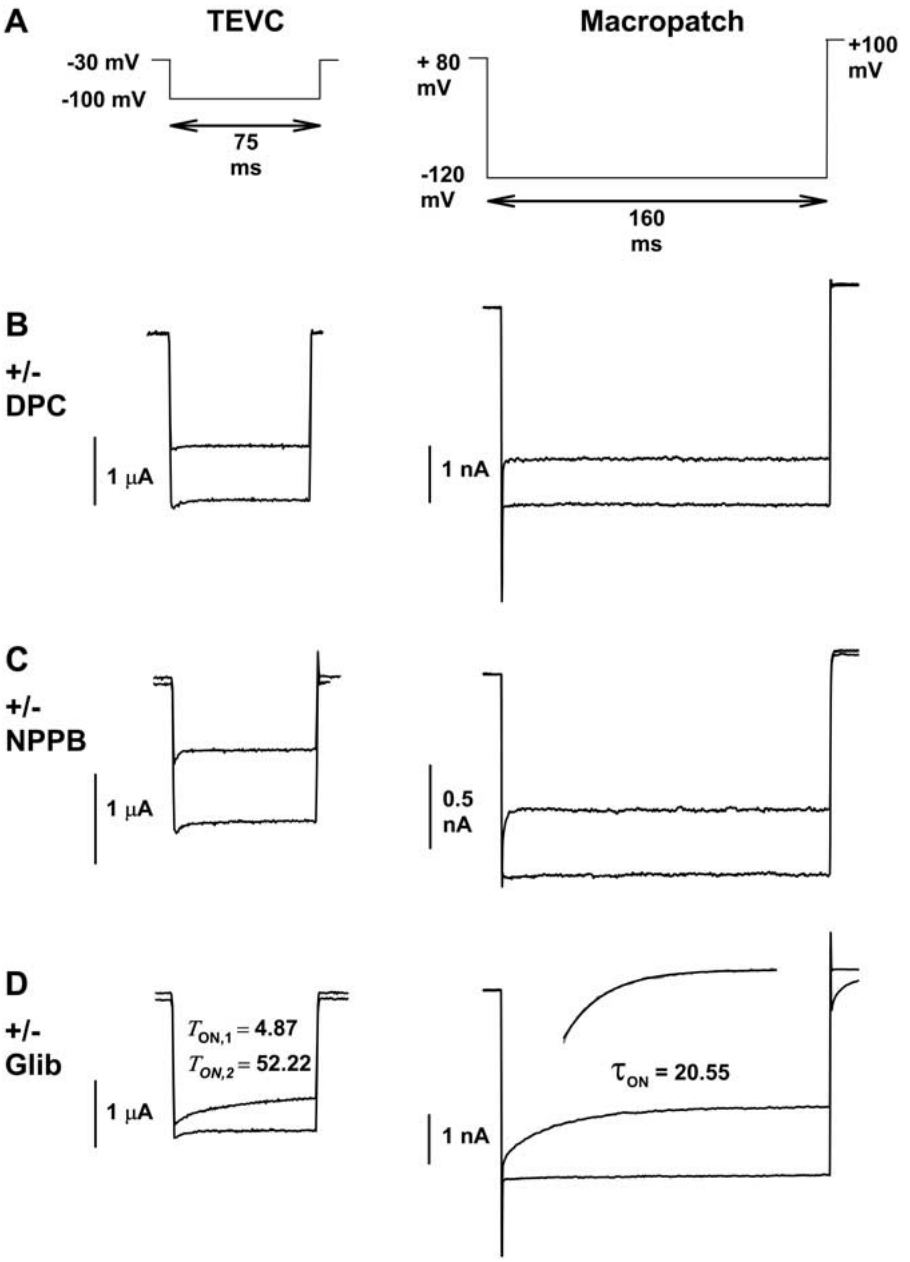

Fig. 3. Comparison of block of CFTR currents in whole-cell (TEVC) experiments (*left*) and inside-out macropatch experiments (*right*). Only those current traces at step potentials of −100 mV (*left*) and −120 mV (*right*) are shown for representative cells using voltage protocols as shown in (*A*). Traces show currents in the absence of drug (*lower traces*) and in the presence of DPC (*B*), NPPB (*C*), and glibenclamide (*D*). For whole-cell data, drug concentration in the extracellular bath was 100 μM. For macropatch data, drug concentrations in the cytoplasmic solution were 100, 50, and 50 μM for DPC, NPPB, and glibenclamide, respectively. Values for time constants shown are in ms for experiments with glibenclamide. The inset in the glibenclamide trace shows the fit (*smooth line*) to the macropatch data (*jagged line*) (correlation coefficient = 0.991).

TEVC experiments is of insufficient duration for steady-state block to be achieved (*see* Methods). However, true forward rates of block were calculated from single-channel experiments described previously (Zhang et al., 2004) and from macropatch recordings described below. At pH 7.5 and V_M = −100 mV, with 100 μM bath glibenclamide, $T_{ON,2}$ was 52.34 ± 1.43 ms (Table 1).

To confirm that these relaxations represent the forward reaction of glibenclamide with the CFTR protein at hyperpolarizing potentials, we studied the dose-dependence of the macroscopic on-rate (the inverse of $T_{ON,2}$). For these experiments, we made use of the enhanced loading of drug at bath pH 6.5 in order to strengthen our ability to fit the relaxations. $T_{ON,2}$ at −100 mV was sensitive to bath drug con-

Table 1. Kinetics of block of macroscopic currents in WT-CFTR

Potential (mV)	Control T_{ON}	Glib, pH 7.5 $T_{ON,1}$	A	$T_{ON,2}$	Glib, pH 6.5 $T_{ON,2}$
−140	5.76 ± 0.45	5.38 ± 0.23	0.21 ± 0.02	50.59 ± 1.75	42.71 ± 2.98
−120	4.74 ± 0.24	4.85 ± 0.30	0.20 ± 0.02	48.06 ± 2.31	39.17 ± 2.64
−100	5.14 ± 0.31	5.02 ± 0.30	0.19 ± 0.02	52.34 ± 1.43	35.92 ± 1.34
−80	5.13 ± 0.29	4.75 ± 0.74	0.16 ± 0.02	47.11 ± 1.87	34.18 ± 3.61
−60	5.44 ± 0.53	5.17 ± 0.65	0.17 ± 0.02	50.09 ± 2.65	34.06 ± 1.21

Kinetics of macroscopic blockade of WT-CFTR were determined by fitting a second-order exponential to the whole-cell currents, measured from TEVC experiments, at each potential to obtain the short (T_{ON}) time-constant of the relaxation under control conditions (pH 7.5) and the short and long ($T_{ON,1}$ and $T_{ON,2}$) time-constants of the relaxation in the presence of 100 μM glibenclamide. Some experiments were performed at pH 6.5, in order to enhance loading of the drug from the bath into the cytoplasm, leading to a faster relaxation at each potential ($P < 0.05$; $n = 4$ - 8). The relative magnitudes of $T_{ON,1}$ and $T_{ON,2}$ did not differ as a function of voltage at pH 7.5 (column "A" expresses the fractional contribution from $T_{ON,1}$).

centration, measuring 51.53 ± 1.88 ms and 35.92 ± 1.34 ms at 25 and 100 μM drug, respectively ($n = 4$–9; $P < 0.001$; Fig. 4*A*). Hence, this component of the relaxation does represent glibenclamide binding to its site(s), and likely reflects interactions with the site that gives rise to the C3 state in single-channel recordings (k_3 in Fig. 1), which is characterized by a slow forward rate. Because we do not know the actual cytoplasmic concentration of glibenclamide in these whole-cell experiments, we will refrain from converting $T_{ON,2}$ into a rate constant. Surprisingly, $T_{ON,2}$ was not voltage-dependent over a narrow range of hyperpolarizing potentials (Fig. 5*A*), although single-channel recordings show that k_3 is significantly voltage-dependent (Zhang et al., 2004). Any voltage-dependence of $T_{ON,2}$ may be obscured by the presence of background block, which confounds the analysis of TEVC currents, or perhaps by contributions from k_1 and k_2 under these conditions.

The Need for a Cleaner Assay

Our ability to quantitatively assay the kinetics of block of macroscopic CFTR currents from measurements of TEVC currents is limited by: i) the presence of background block, arising from a constituent of oocyte cytoplasm; ii) the short duration of voltage pulses that are tolerated by whole oocytes under TEVC; and iii) the inability to accurately control cytoplasmic glibenclamide concentration, since glibenclamide equilibrates slowly and incompletely between bath and the oocyte interior. In order to overcome these limitations, we turned to excised, inside-out macropatches expressing large numbers of CFTR channels that were activated by exogenous PKA in the presence of 1 mM MgATP. All currents described here represent currents in 1 mM MgATP *after* the fast rundown that often occurs following washout of PKA. Since macropatches can be held at extreme voltages for hundreds of milliseconds, we

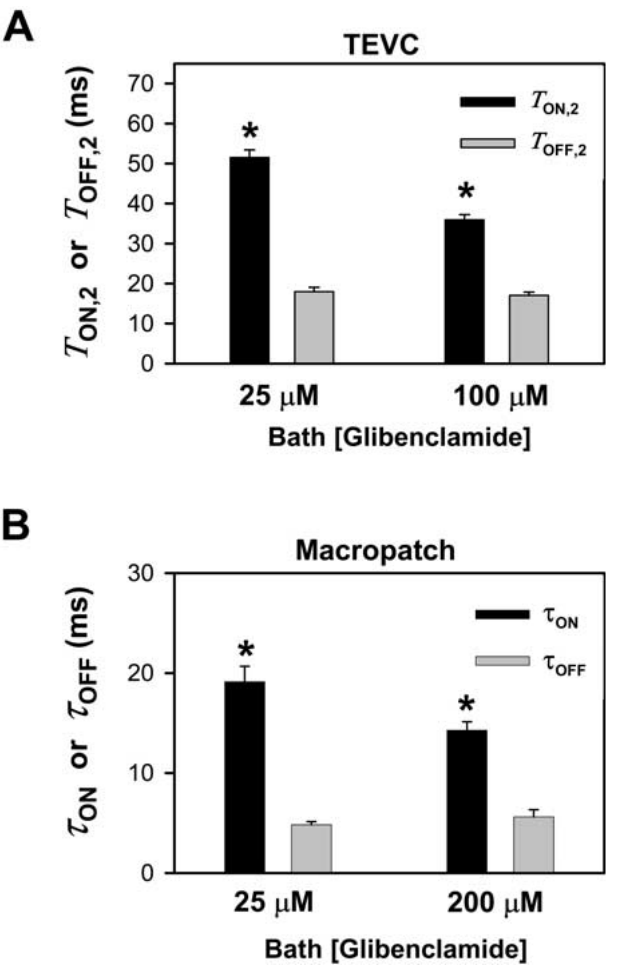

Fig. 4. (*A*) Concentration dependence of the time constants for macroscopic block ($T_{ON,2}$) and relief from block ($T_{OFF,2}$) from TEVC currents was determined at 25 and 100 μM bath [glibenclamide], with bath pH 6.5. Data shown are mean ± SE for $n = 4 - 5$ experiments. (*B*) Similar results describe the kinetics of macroscopic current block (τ_{ON}) and relief from block (τ_{OFF}) for macropatch experiments, with bath pH 7.5. Only the time constants for the forward reaction ($T_{ON,2}$ and τ_{ON}) were concentration-dependent (*$P < 0.001$), confirming that these time constants reflect the forward and reverse reactions of glibenclamide with CFTR, respectively.

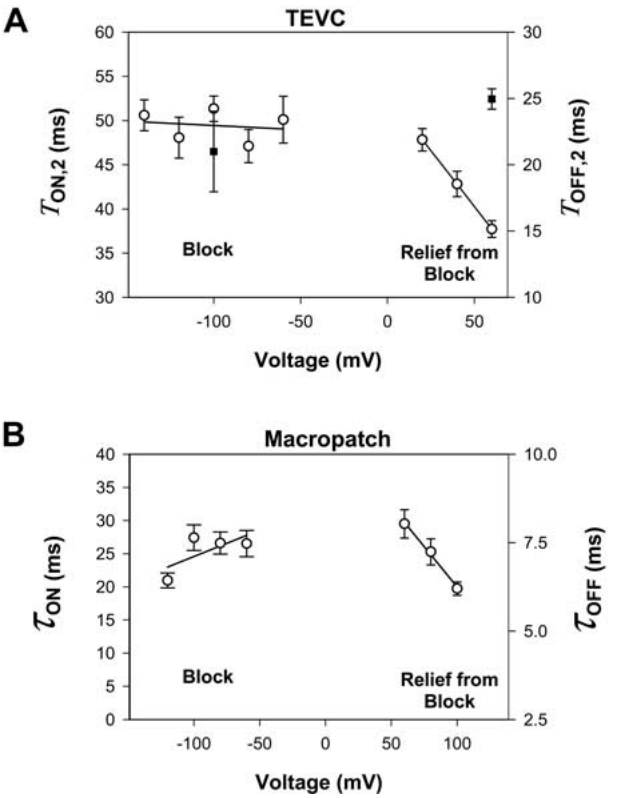

Fig. 5. Effects of voltage on macroscopic kinetics for block of WT-CFTR by glibenclamide. (*A*) In TEVC experiments, $T_{OFF,2}$ was linearly related to membrane potential, while $T_{ON,2}$ was not. $T_{OFF,2}$ was also increased at +60 mV in the presence of a reduced driving force for Cl^- entry. *Empty circles*: Standard bath solution with 100 mM Cl^- *Filled squares*: Bath solution with 10 mM Cl^-. Points represent mean ± SE for $n = 4 - 9$ oocytes in each condition. (*B*) Similar results in macropatch experiments.

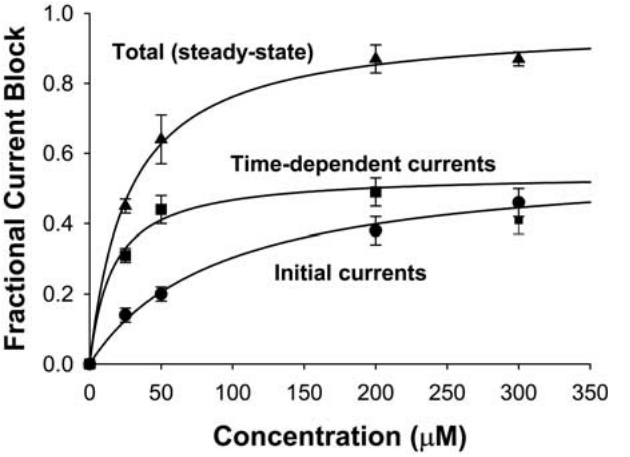

Fig. 6. Concentration dependence of block of initial currents (*circles*), time-dependent currents (*squares*), and steady-state currents (*triangles*) in macropatch experiments. Data shown are mean ± SEM for $n = 5 - 8$ experiments at each concentration, and were fit with a Michaelis-Menten function (r^2 values between 0.92 and 0.99).

were able to apply voltage pulses longer in duration than those used in TEVC. Under these conditions, block by glibenclamide and relief from block reached steady state, allowing us to quantify more accurately the time constants describing these relaxations. Background block due to the cytoplasmic constituent does not exist in excised macropatch records; currents at hyperpolarizing potentials are not time-dependent in the absence of exogenously supplied blocker. Finally, we were able to accurately control glibenclamide concentration, since the drug was being applied directly to the cytoplasmic surface. Solutions were exchanged by a fast perfusion system, allowing comparison of currents in the presence and absence of drug while limiting rundown of CFTR activity.

Macropatch Currents

Figure 3 (*right*) shows macropatch currents at hyperpolarizing potentials with and without added blockers. In the absence of blocker, CFTR macropatch currents were time-independent. In the presence of 100 μM DPC, CFTR macropatch currents remained time-independent although the steady-state current was inhibited compared to control; block by 50 μM NPPB proceeded with a slight degree of time dependence, due to interactions with the site that results in longer closed times for this drug (~2 ms; Zhang et al., 2000a) than for DPC. The limited time-dependence of block in the presence of DPC or NPPB is consistent with the notion that the fast blocking kinetics for these two drugs are too fast to be resolved by macropatch current measurements.

In contrast, macropatch currents measured in the presence of 50 μM glibenclamide exhibited the following two features (Fig. 3*D right*). First, the peak current measured immediately following the jump to a hyperpolarizing potential was reduced. The magnitude of this initial block was dependent upon glibenclamide concentration (Fig. 6). Hence, this rapid phase of inhibition by glibenclamide likely reflects interactions with the sites underlying the C1 and C2 states (k_1 and k_2 in Fig. 1); rundown may also make a small contribution. Following the inhibition of peak currents, CFTR macropatch currents in the presence of glibenclamide exhibited a slow relaxation, which was fit best by a first-order exponential function. The time constant describing this relaxation (τ_{ON}) was concentration-dependent (Fig. 4*B*); hence, this likely reflects the transition labeled k_3 to the C3 state in Figure 1. In accordance with the results from TEVC experiments, τ_{ON} from macropatch experiments did not exhibit significant voltage dependence (Fig. 5*B*). The site underlying the time-dependent component of block exhibited greater affinity for glibenclamide than did the site(s) underlying initial block (Fig. 6). The k_d for block of initial currents was 91.4 ± 15.7 μM, while the k_d for block of the time-dependent com-

ponent was 16.1 ± 4.7 μM. This is consistent with the 8-fold difference in K_ds for interactions at the C2 and C3 states determined from single-channel kinetics (Zhang et al., 2004). The overall K_d for block of steady-state macroscopic currents was 27.3 ± 2.3 μM.

Kinetics of Relief from Block at Depolarizing Potentials

TEVC Currents

Glibenclamide, DPC, and NPPB block CFTR channels effectively only at hyperpolarizing membrane potentials (McCarty et al., 1993; Zhang et al., 2000a; Zhou Hu & Hwang, 2002; Zhang et al., 2004); at depolarizing membrane potentials, these drugs rapidly dissociate from their binding sites. In the case of the arylaminobenzoates, which block CFTR TEVC currents with very low affinity at $V_M = -100$ mV (K_ds of ~200 and ~100 μM, respectively, for DPC and NPPB), the off-rates are so rapid that no relaxations were evident following a voltage jump to depolarizing potentials (Fig. 7*B*,C *left*); the current immediately returned to control amplitude. In oocytes exposed to glibenclamide, however, the relief from block was complex (Fig. 7*D*). Initial currents just after the voltage step were decreased in a glibenclamide concentration-dependent manner; at $V_M = +60$ mV and pH 6.5, initial currents were decreased 5.8 ± 1.03% with 25 μM glibenclamide and 38.8 ± 3.3% with 100 μM bath glibenclamide ($n = 5$; $P < 0.001$). The rapid rise in current to this level represents relief from block in the C1 and C2 states ($k_{-1}$and k_{-2} in Fig. 1). From our single-channel studies with 25 μM cytoplasmic glibenclamide (Zhang et al., 2004), we know that k_{-1} and k_{-2} are 4,000 s^{-1} and 510s^{-1}, respectively. These reverse rate constants for glibenclamide are very similar to the reverse rates for unbinding of DPC (2,500 s^{-1}; McCarty et al., 1993) and NPPB (483 s^{-1}; Zhang et al., 2000a). This early phase of relief from block by glibenclamide, therefore, is too rapid to be resolved by macroscopic recordings.

Following the rapid release of glibenclamide from the sites underlying the C1 and C2 states, TEVC currents exhibited a slow relaxation toward control current levels, which was fit best by a second-order exponential. The faster component of the relaxation ($T_{OFF,1}$) was not dependent upon glibenclamide concentration. Instead, this component of the relaxation appears to be due to relief from block by the same cytosolic component that induces an inhibitory relaxation at negative potentials in the absence of added drug (Fig. 3); the off-rate of this background blocker (k_{-B} in Fig. 1) is rapid in the absence but slowed in the presence of glibenclamide, suggesting that the two blocking molecules may interact in the channel pore. The more prominent slow component of the off-relaxation arises from relief from block by glibenclamide at the site underlying the C3 state. This rate constant (k_{-3}) and its relevant macroscopic time-constant ($T_{OFF,2}$) also were not dependent upon glibenclamide concentration. Figure 4*A* shows that $T_{OFF,2}$ at +60 mV was insensitive to bath-applied drug concentration (17.98 ± 1.06 ms and 17.04 ± 0.80 ms at 25 and 100 μM, respectively; $n = 4-5$; $P = 0.52$). However, $T_{OFF,2}$ was quite voltage-dependent (Fig. 5*A*). At pH 7.5, the magnitude of unrecovered current at the end of the voltage pulse was variable, and not sensitive to glibenclamide concentration; this likely reflects a combination of rundown and the consequence of using a brief voltage-jump duration.

To confirm that the slow relaxation reflects dissociation of glibenclamide from the site corresponding to the C3 state, we asked whether the time constant describing this relaxation was affected by a change in the driving force for chloride. With bath [Cl^-] reduced to 10 mM (Fig. 5*A*), $T_{OFF,2}$ at +60 mV was increased from 15.15 ± 0.63 ms to 24.96 ± 0.77 ms ($n = 8$; $P < 0.001$). This likely represents a relationship between the degree of occupancy of chloride-binding sites and the stability of glibenclamide at its binding site(s) in the pore (Goldstein & Miller, 1991; Zhou et al., 2002). This is consistent with the increase in the equivalent time constant from our single-channel studies upon tenfold reduction of external [Cl^-], where $1/k_{-3}$ changed from 38 ms to 184 ms (Zhang et al., 2004). For the macroscopic kinetics at depolarizing potentials, the dependency upon the permeant anion driving force confirms that the slow relaxation reflects relief from glibenclamide-induced block, and represents exit from the C3 state that is characterized by a slow microscopic off-rate.

Macropatch Currents

To avoid complications inherent in analysis of TEVC currents, we also assayed relief from glibenclamide-induced block using inside-out macropatches (Fig. 7 *right*). In the absence of added blocker, macropatch currents at depolarizing potentials exhibited no time-dependence. In the presence of DPC or NPPB, which block effectively only at negative potentials, currents at positive potentials were the same as controls, reflecting rapid dissociation of these drugs from their binding sites. In the presence of 50 μM cytosolic glibenclamide, initial currents immediately following the voltage jump were decreased by 40.7 ± 2.6 % ($n = 6$); the rapid rise in current to this level likely reflects loss of glibenclamide from the C1 and C2 states, as seen in the TEVC recordings.

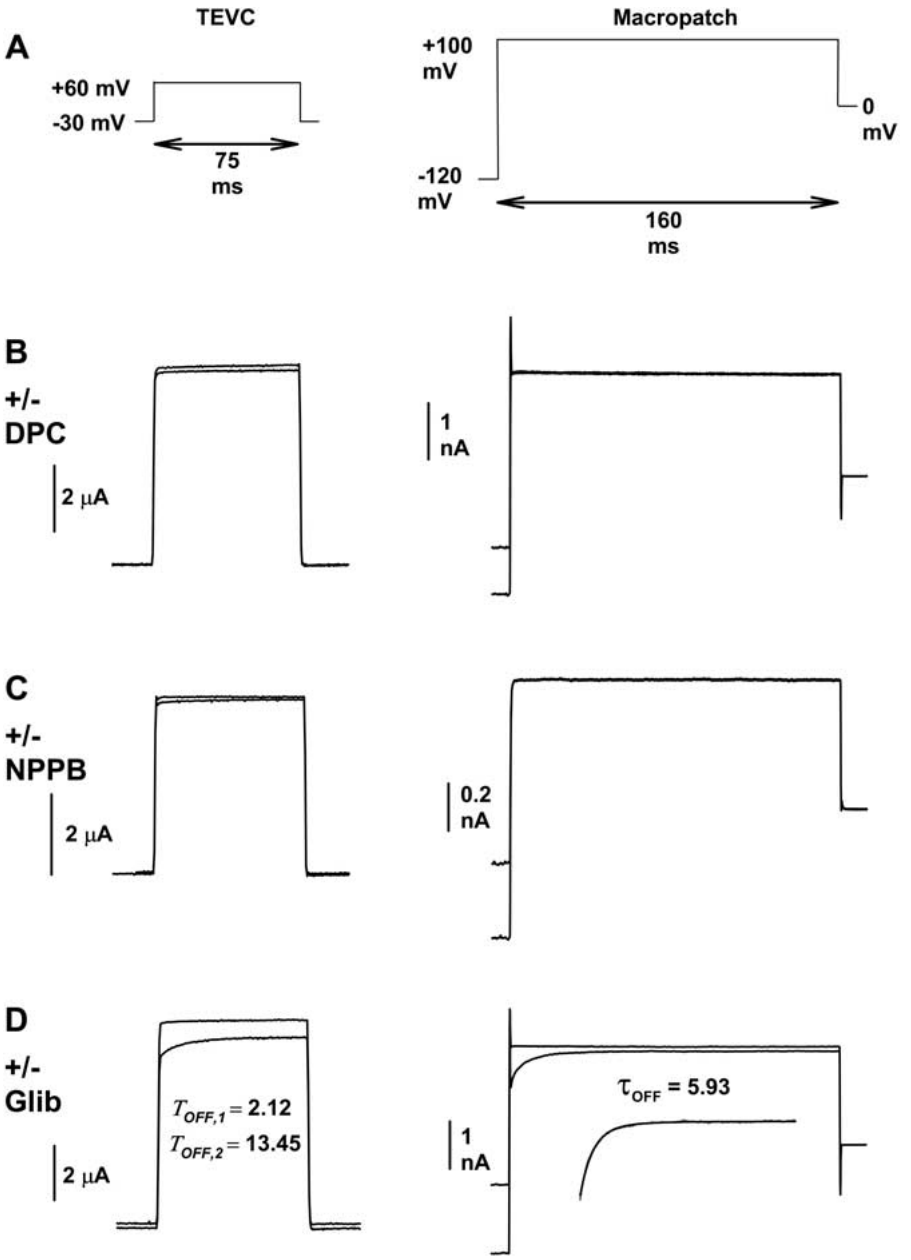

Fig. 7. Comparison of relief from block of CFTR currents in whole-cell (TEVC) experiments (*left*) and inside-out macropatch experiments (*right*). Only those current traces at step potentials of +60 mV (*left*) and +100 mV (*right*) are shown for representative cells using voltage protocols as shown in (*A*). Traces show currents in the absence of drug (*upper traces*) and in the presence of DPC (*B*), NPPB (*C*), and glibenclamide (*D*), at the same concentrations as in Fig. 3. Values for time constants shown are in ms for experiments with glibenclamide. The inset in the glibenclamide trace shows the fit (*smooth line*) to the macropatch data (*jagged line*) (correlation coefficient = 0.993).

Following the rapid phase of relief from block, macropatch currents exhibited a slow relaxation that was fit best with a first-order exponential function, reflecting the k_{-3} transition away from the C3 blocked state. The rate constant was not sensitive to glibenclamide concentration (Fig. 4*B*), but did exhibit significant voltage dependence (Fig. 5*B*). The magnitude of unrecovered current at the end of the voltage pulse was variable, and not sensitive to glibenclamide concentration. Hence, the slow relaxation at depolarizing potentials in macropatch currents likely represents dissociation of the drug from the site corresponding to the C3 state that we observed in single-channel studies (Zhang et al., 2004).

Shifts in Voltage Dependence of Blockade

The data presented above, both from glibenclamide-mediated block of TEVC currents and from glibenclamide-mediated block of macropatch currents, suggest that block occurs in two phases at negative membrane potentials. The early phase of block represents occupancy of the C1 and C2 states, which occurs with rapid kinetics in single-channel studies (Zhang et al., 2004). The late phase of block represents the occupancy of the C3 state, which occurs with slow kinetics in single-channel studies. Because block at C1 + C2 occurs with low affinity and low voltage dependence, while block at C3 occurs with higher affinity and significant voltage dependence, we

might expect to observe shifts in the affinity and voltage dependence of block during a jump to negative potentials. We investigated this possibility by calculating the apparent K_d at several potentials, using TEVC currents measured in the presence of 100 μM glibenclamide, and separately assaying block of early-phase currents (average currents in the first two ms following each voltage step) and block of late-phase currents (average currents in the final ten ms at each potential). These results are summarized in Fig. 8. We did not calculate the voltage dependence of block using Woodhull analysis because a major assumption of the Woodhull model is that the voltage dependence of block represents the voltage dependence of equilibration with a single binding site; as stated previously, our data are consistent with multiple glibenclamide binding sites in the pore of CFTR.

Fast block of CFTR TEVC currents resulted in an apparent K_d of 405.5 ± 3.9 μM at $V_M = -100$ mV ($n = 9$). In contrast, late-phase block of TEVC currents resulted in an apparent K_d of 246.6 ± 4.6 μM at $V_M = -100$ mV ($P < 0.005$ compared to early phase). However, the extrapolated K_ds at 0 mV were nearly identical for early- and late-phase block (759.7 and 717.9 μM, respectively). In other words, the slope of the relationship between voltage and apparent affinity changed between early-phase and late-phase block, while the intercept at 0 mV did not change significantly (Fig. 8). This indicates that the improvement in block of inward currents during the voltage step does not simply represent a change in affinity. Rather, both the voltage dependence of block and the apparent affinity at negative potentials changed through time. Hence, the shallow (but non-zero) voltage dependence of block for early-phase (peak) currents following voltage steps from a holding potential of −30 mV may largely represent the weakly voltage-dependent interactions between glibenclamide and the C1 and C2 states. Following a step in membrane potential, the current relaxes slowly toward its new steady-state value in the presence of drug, representing interactions with a site that exhibits stronger voltage dependence. That the voltage dependence of late-phase block differs from that of early-phase block may represent a shift in the occupancy of the two pore-domain binding sites identified in excised single-channel patch experiments (Zhang et al., 2004).

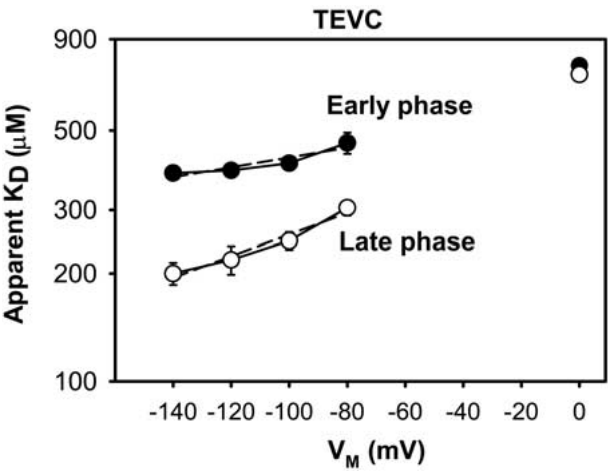

Fig. 8. The voltage dependence of block of whole-cell CFTR currents by glibenclamide is time-dependent. Voltage dependence of block by 100 μM glibenclamide, measured during the first 2 ms (*Early phase*) and last 10 ms (*Late phase*) of a 75 ms step to each voltage. Apparent K_D at each voltage was determined for inward currents using Eq. 1. Points are mean ± SD for $n = 9$ oocytes. Dashed lines are from linear regression. The points at 0 mV are the mean ± SD of the *y*-intercept from linear regression of the data between −140 and −80 mV.

Summations of Single-Channel Recordings

In both whole-cell and macropatch experiments, time-dependent inhibition was observed when V_M was pulsed from a holding potential where glibenclamide block is weak to a hyperpolarizing potential where the affinity for drug binding is stronger. Initial currents were inhibited rapidly, leading to a reduction in peak current, and this was followed by a slower relaxation reflecting glibenclamide-induced current decay. The fact that this development of block is biphasic suggests the interaction between glibenclamide and multiple binding sites. This is consistent with the analysis of steady-state single-channel kinetics (Zhang et al., 2004), which revealed three distinct glibenclamide-induced intraburst closed states, C1 – C3, varying in duration from < 1 ms to ~40 ms.

To correlate the single-channel kinetic parameters with the macroscopic behavior we used summations of multiple single-channel bursts (*see* Colquhoun & Hawkes, 1995). The first 200 ms of multiple CFTR bursts at $V_M = -100$ mV were summated in the presence and absence of 25 μM glibenclamide at cytosolic pH 7.3 (data are from Zhang et al., 2004). To avoid confusion between long blocked states and interburst closed states, only those bursts that were preceded by more than 1 s at the closed current level were used in this analysis. Furthermore, only bursts lasting longer than 200 ms were included so that we could be certain that gating termination of a channel burst (i.e., an NBD-mediated channel closure) did not contaminate the current summations.

Single-channel summations were characterized by a rapid, monophasic decay in the absence of blocker and a biphasic decay in the presence of glibenclamide (Figs. 9*A* and *B*). Immediately following the initiation of CFTR bursts, the summed current is at a maximum; current then decays rapidly to a lower steady state. The time constant for the fast current decay (τ_{s1}) was 2.94 and 2.95 ms in the absence and presence of glibenclamide, respectively. This can be

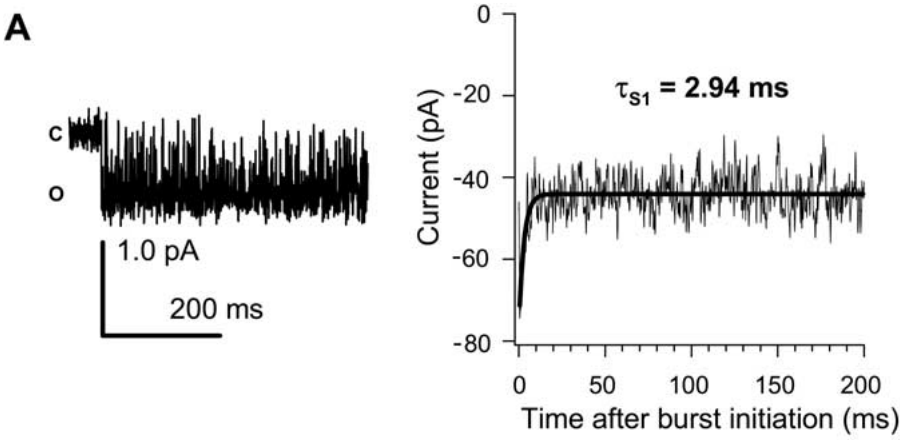

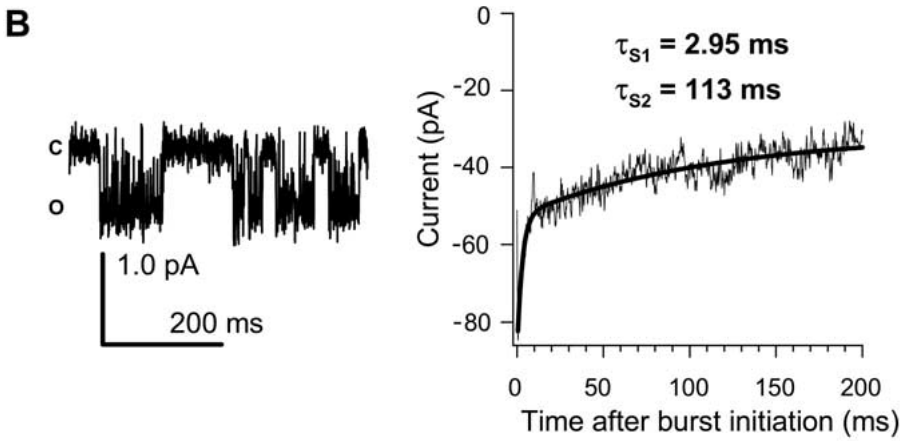

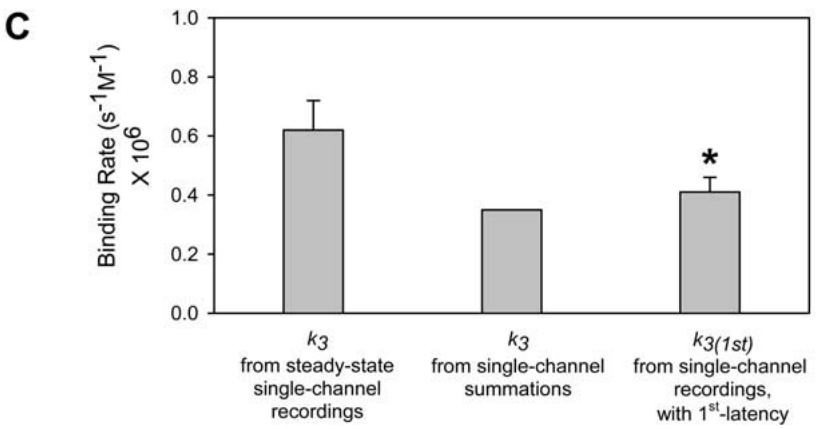

Fig. 9. Decay of summations of multiple single-channel bursts in the absence and presence of glibenclamide. (*A*) The first 450 ms of an open-channel burst in the absence of blocker (*left*) shows only rapid block of the pore by the intracellular buffer. A monophasic decay was observed in the current summation (*right*) of the first 200 ms of 82 open-channel bursts in the absence of blocker, at V_M = −100 mV. At the initiation of a burst, current rises to a maximum, and then decreases due to background block, which then occurs at a constant rate. This results in a single-exponential fit of the summation. (*B*) The first 450 ms of an open-channel burst in the presence of 25 μM glibenclamide (*left*) shows both the brief and long-lived drug-induced closed states, as well as rapid block of the pore by the intracellular buffer. A biphasic decay was observed in the current summation (*right*) of the first 200 ms of 96 open channel bursts in presence of glibenclamide due to the addition of slow transitions to the C3 state. (*C*) Glibenclamide binding rates to the long blocked state (C3 state) calculated from steady-state single-channel intraburst kinetics (from Zhang et al., 2004), slow decay of single-channel current summations (calculated as $1/\tau_{s2}$), and first latency to long block in single-channel recordings (*$p < 0.05$, compared to steady-state k_3).

attributed to the flickery intraburst blockade events (C_B state in Fig. 1), observed even in the absence of exogenously-applied blocker, which arise from block of the pore by the pH buffer TES used in our intracellular solutions (Zhang et al., 2004), and results in a closed dwell time very similar to that of the C1 state. In the presence of glibenclamide, the fast component of decay also reflects binding of glibenclamide to the C1 and C2 states, which also have fast on-rates and short durations. The time-constant for the slower decay in the presence of glibenclamide (τ_{S2}) was 113 ms. This second component arises from the additional process of glibenclamide binding to the site that produces the long glibenclamide-induced C3 closed state, because the frequency of transitions to the C3 state is low, while the duration of the C3 state is substantial (~40 ms; Zhang et al., 2004) (e.g., Fig. 9*B left*).

While the slow nature of the second component of the biphasic decay observed in both macroscopic currents and summations of single-channel bursts is qualitatively consistent with the slower on-rate of glibenclamide to induce the long blocked state (k_3 in Fig. 1), there appears to be some inconsistency between k_3 derived from the steady-state single-channel kinetics ($k_3 = 0.62 \pm 0.10 \times 10^6$ $s^{-1}M^{-1}$; Zhang et al., 2004) and k_3 derived from the summations of single-channel bursts ($k_3 = 1 / \tau_{S2} = 0.35 \times 10^6$ s^{-1} M^{-1}; Fig. 9*C*). One possible explanation for this discrepancy is that k_3 is slower at the beginning of a channel burst, as suggested by the representative trace shown in Fig. 9*B* (*left*).

To test the hypothesis that glibenclamide binds more slowly after the initial opening of a channel compared to later in a burst we measured the initial on-rate ($k_{3\ (1st)}$; the inverse of first latency) to closings longer than 10 ms; this threshold was used to discriminate glibenclamide-induced intraburst blocked states (C_1 or C_2) and longer blocked states (C3) (*see* Zhang et al., 2004). The calculated value for $k_{3\ (1st)}$ was $0.41 \pm 0.05 \times 10^6$ s^{-1} M^{-1} ($n = 12$). Hence, the first latency to long closings measured from multiple bursts in each patch was significantly longer ($P < 0.05$) than predicted by the overall on-rate to long closings, by an average difference of (1.67 ± 0.33) fold ($n = 12$). Along with the summations of single-channel bursts, this suggests that once the channel opens, the initial binding of glibenclamide to the site responsible for the long blocked state (C3) is slower than subsequent bindings within the open channel (Fig. 9*C*). These results may explain why the on-rate to long closings calculated from single-channel summations, which are impacted heavily by first latency effects, is lower than the on-rate calculated from steady-state analysis of single-channel kinetics. They also suggest that glibenclamide's access to at least this one binding site is state-dependent.

Table 2. Macroscopic kinetics show interaction between glibenclamide and DPC

	WT-CFTR	
	Glyb	Glyb + DPC
$T_{ON,2}$	52.17 ± 2.32[a]	38.28 ± 4.35
$T_{OFF,2}$	14.92 ± 0.84[b]	25.08 ± 1.79

Kinetics of macroscopic block ($T_{ON,2}$) and macroscopic relief from block ($T_{OFF,2}$) in TEVC experiments were determined from voltage jumps to −100 mV and +60 mV, respectively, in oocytes expressing WT-CFTR. Blockade was first assessed in the presence of 100 μM glibenclamide, then in the presence of glibenclamide plus 200 μM DPC. Comparisons are by paired *t*-test. ($n = 5$ for each combination;
[a] $P = 0.024$;
[b] $P = < 0.002$

Glibenclamide and DPC Interact in the Pore

Our previous experiments showed that patches studied in the concurrent presence of glibenclamide and DPC exhibited an increase in the overall blocking rate, reflected as a decrease in the open dwell-time duration, and a decrease in the rate of relief from block at the C3 state (k_{-3}), without a change in the rate of relief from block at the C1 or C2 state (Zhang et al., 2004). As a final test of the multistate model, we asked whether the kinetics of glibenclamide-induced block and relief from block of macroscopic currents would be affected by the concurrent presence of DPC in the same way that the kinetics of single-channel block were. We addressed this question in whole-cell CFTR currents by taking advantage of the large differences in the kinetics of block and relief from block in the presence of these two drugs, kinetics for DPC being far faster than those for glibenclamide. For these experiments, after assessing blockade in the presence of 5 μM ISO + 100 μM glibenclamide, oocytes were incubated for 7 min in solution containing 5 μM ISO + 100 μM glibenclamide + 200 μM DPC.

As described above, macroscopic currents in WT-CFTR were blocked slowly by 100 μM glibenclamide, with a mean time-constant $T_{ON,2}$ at −100 mV of 52.17 ± 2.32 ms (Table 2). Block of macroscopic currents by DPC is essentially instantaneous — too fast to be fit accurately (Zhang et al., 2000a; Fig. 3). In the presence of two blockers of CFTR, one would expect that the magnitude of block would be increased simply because this is dependent upon blocker concentration. However, rapid block by DPC in the presence of glibenclamide would be expected to reduce the peak currents, as DPC rapidly equilibrates with its binding site, but should only affect the time dependence of inhibition by glibenclamide if DPC and glibenclamide were to interact in the pore. Consistent with this notion, we found that in the concurrent presence of 100 μM glibenclamide

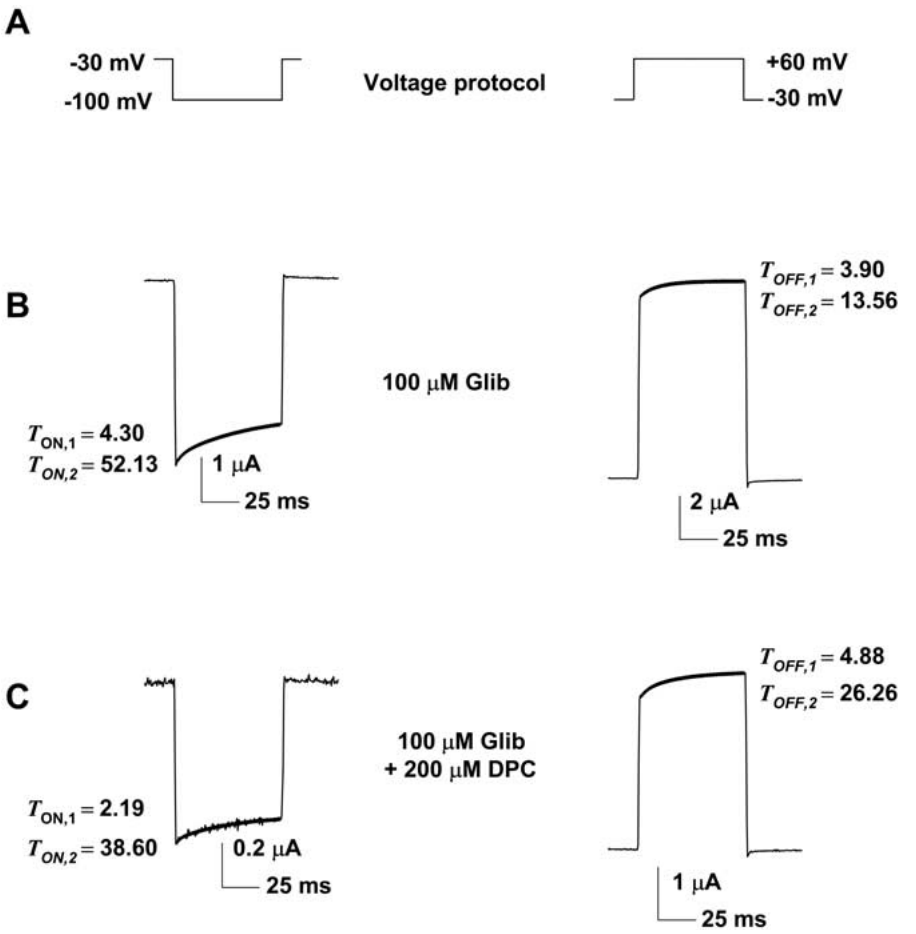

Fig. 10. Glibenclamide and DPC interact in the pore. Kinetics of macroscopic block (*left*) and relief from block (*right*) were determined in WT-CFTR from TEVC experiments as described for Fig. 3 and Fig. 7. Voltage protocols are shown in (*A*), Kinetics were first measured in the presence of 100 μM glibenclamide (Glib) (*B*), and then in the concurrent presence of glibenclamide plus 200 μM DPC (*C*). Data shown are for a representative cell. Values for the time constants listed are in ms. The thick line shows exponential fit to the data.

and 200 μM DPC, $T_{ON,2}$ was reduced to 38.28 ± 4.35 ms (n = 5; p = 0.02 by paired t-test; Table 2 and Fig. 10*C left*). This effect could result from DPC enhancing the on-rate of glibenclamide to its binding site or from DPC reducing the off-rate of glibenclamide from its binding site. Indeed, addition of DPC clearly slowed the relief from block associated with the k_{-3} transition, as $T_{OFF,2}$ was increased from 14.92 to 25.08 ms (Fig. 10*C right*; Table 2). We cannot ignore the possibility that glibenclamide interferes with the rapid equilibration of DPC with its binding site; however, we would expect that this would result in a decreased on-rate of macroscopic block rather than an increase as shown here.

To distinguish between effects of DPC on the macroscopic glibenclamide on- and off-rates, we utilized single-channel summations. Figure 11 shows that while the first time constant of the decay in the summed single-channel currents was reduced by the concurrent presence of DPC and glibenclamide, likely due to the very rapid on-rate of DPC to its binding site (~6×10^7 M^{-1} s^{-1}; McCarty et al., 1993), the second time constant was not different compared to experiments with glibenclamide alone (Fig. 9). This makes it unlikely that the effect of DPC on macroscopic block by glibenclamide is due to enhancement of the glibenclamide on-rate. Paired single-channel experiments at V_M = −100 mV in our previous studies indicated that only the off-rate of glibenclamide from the C3 state (k_{-3}), and not the on-rate to this state or the rates to or from states C1 or C2, was sensitive to interaction with DPC (Zhang et al., 2004). Taken together, these data show that DPC is capable of reducing the dissociation of glibenclamide from one of its binding sites, at both hyperpolarizing and depolarizing potentials. The glibenclamide-binding site affected by DPC is the site that interacts with glibenclamide with slow kinetics, resulting in the C3 state.

Hence, data from TEVC currents, single-channel summations, and steady-state single-channel experiments (Zhang et al., 2004) indicate that the off-rate

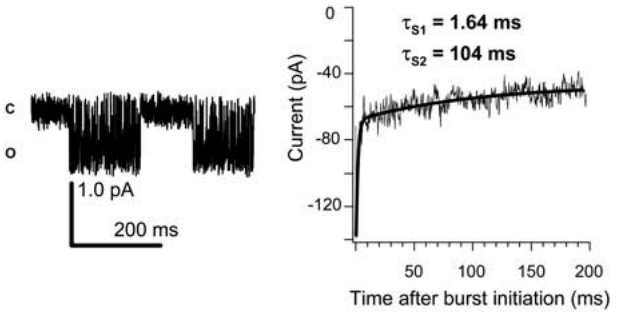

Fig. 11. Summation of multiple single-channel bursts in the presence of glibenclamide plus DPC. The first 450 ms of an open-channel burst in the presence of 25 μM glibenclamide plus 100 μM DPC (*left*) shows both the brief and long-lived drug-induced closed states, as well as rapid block of the pore by the intracellular buffer. A biphasic decay was observed in the current summation of the first 200 ms of open channel bursts in the presence of glibenclamide plus DPC in the intracellular solution (*right*). The first 200 ms of 153 bursts at $V_M = -100$ mV were used for this summation.

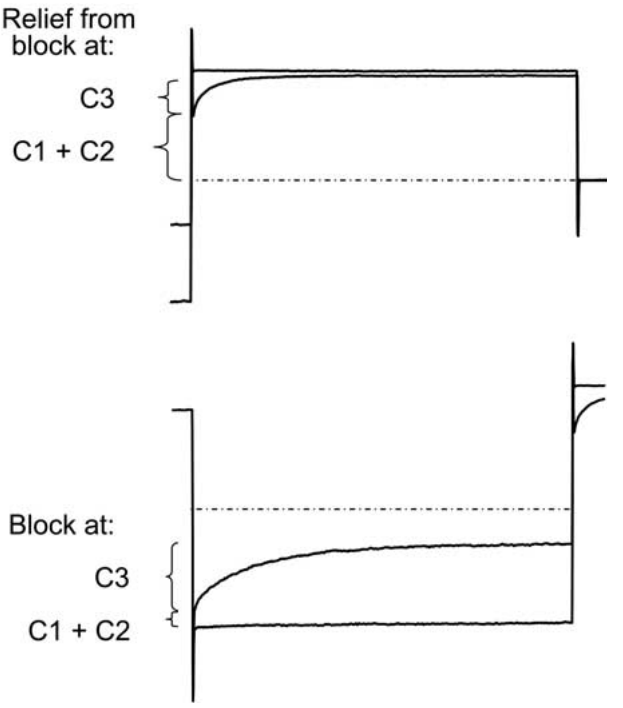

Fig. 12. Using macroscopic kinetics to study microscopic interaction rates. The biphasic time course of block (*lower panel*) and relief from block (*upper panel*) in macropatch experiments, using voltage protocols as shown in Figs. 3 and 7, are proposed to reflect interactions with different glibenclamide-binding sites, C1 – C3, which differ in kinetics at the single-channel level. Dashed line represents the zero current level.

from one of the glibenclamide-induced intraburst closed states was reduced in the concurrent presence of DPC. The observation that the kinetics of block by glibenclamide can be altered by the concurrent presence of DPC indicates that the cytoplasmic vestibule of CFTR, which forms the pathway for movement of these intracellular drugs to their binding sites in the pore and back out again, is quite large, since both drugs, along with water and Cl^-, can occupy the pore and/or the inner vestibule at the same time (Linsdell & Hanrahan, 1996; Zhou et al, 2002; Zhang et al., 2004).

Discussion

We recently described experiments in which we investigated the steady-state block by glibenclamide of single WT-CFTR channels in excised patches (Zhang et al., 2004). That study identified multiple glibenclamide-induced closed/blocked states (C1, C2 and C3) with varying microscopic kinetics, voltage-dependencies, and pH-dependencies. The proposed multi-state model (Fig. 1) predicts that block of macroscopic currents should be complex. Previous studies of glibenclamide-mediated blockade of CFTR, using either whole-cell recording or single-channel recording, did not indicate this complexity. Hence, we used two-electrode voltage clamp, macropatch recordings, and summations of single-channel currents to study the effects of glibenclamide on macroscopic currents from CFTR expressed in oocytes, to test the predictions of our model. We show that glibenclamide blocks CFTR macroscopic currents by a complicated mechanism, which we hypothesize likely arises from interaction with multiple binding sites with different pH- and voltage-dependencies and different affinities for the drug. This conclusion is consistent with previous work by Sheppard and colleagues (Cai, Lansdell & Sheppard, 1999) who, based upon the effects of the non-sulfonylurea hypoglycemic agent meglitinide, speculated that glibenclamide interacts with more than one site in the CFTR pore.

Macroscopic Current Blockade by Glibenclamide is Time-dependent

A principal finding in this study is that glibenclamide blocked macroscopic CFTR currents with slow kinetics. Unblocked macroscopic currents in WT-CFTR and nearly all mutants studied to date are time-independent (exceptions are S1118F-CFTR and V317E-CFTR, which confer voltage-jump relaxations on currents in the absence of added blockers; Zhang, McDonough & McCarty, 2000b; Zhang et al. 2002). Blockade by the arylaminobenzoates DPC and NPPB occurs very rapidly and does not induce significant time-dependence (McCarty et al., 1993; Zhang et al., 2000a). However, both the macroscopic on-rate and off-rate for the interaction of glibenclamide with CFTR were slow, resulting in pronounced time dependence of block of both whole-cell CFTR

currents and currents from excised, inside-out macropatches.

The whole-cell current relaxations at both hyperpolarizing and depolarizing potentials were fit best with a second-order exponential. The shorter exponential at hyperpolarizing potentials may reflect a combination of: 1) fast block of CFTR by cytosolic components (McCarty et al., 1993), as seen in the absence of exogenous blocker, and 2) block of CFTR by interaction of glibenclamide with a binding site or sites characterized by a fast on-rate. The longer exponential at $V_M = -100$ mV may reflect interaction of glibenclamide with a binding site characterized by a slower on-rate. The macroscopic time-constant at hyperpolarizing potentials was sensitive to drug concentration and the macroscopic time constant at depolarizing potentials was sensitive to external [Cl^-], confirming that these relaxations predominantly reflect the forward and reverse reactions between drug and receptor at hyperpolarizing and depolarizing potentials, respectively. The voltage-dependent nature of blockade appears to arise from a voltage dependence of the off-rate, because the time constant for the macroscopic relief from block at depolarizing potentials was voltage-dependent, while the time constant for macroscopic block at hyperpolarizing potentials was not. This likely reflects knockoff of drug from its binding site by Cl^- entry, as the off-rate is sensitive to the driving force for Cl^-.

Due to the complications arising from time-dependent block of CFTR currents by a component of the oocyte cytoplasm in TEVC experiments, we asked whether the complex kinetic behavior of block by glibenclamide was evident in macropatches, in which we could more easily control both activation state and exposure to drug at known concentrations. In these experiments, distinctions were more easily made between rapid block by DPC and NPPB and block by glibenclamide, at least part of which is slow. The latter clearly interacted with the pore in a biphasic manner, exhibiting rapid, time-independent block immediately after a voltage pulse to hyperpolarizing potentials and slow, time-dependent block thereafter.

It is clear from the TEVC data shown in Fig. 8 that both the apparent affinity for glibenclamide and the voltage-dependence of block by glibenclamide increased through time. Similarly, macropatch data shown in Fig. 6 indicate that the apparent affinity for the fast, time-independent component of block was lower than that for the time-dependent component of block. Also, the voltage-dependence of the relaxations at depolarizing potentials, due to relief from block, in both TEVC and macropatch currents are consistent with the voltage-dependence of the duration of the C3 state in single-channel recordings (Zhang et al., 2004).

Macroscopic voltage-jump relaxations of this sort usually reflect voltage-dependent changes in the fraction of time that a channel spends in various states. Hence, the time-dependence of blockade may describe a sequence of states of the channel with varying affinity (Dawson, 1996). If the glibenclamide-induced relaxations are, as we propose, due to time-dependent interactions of glibenclamide with two or more binding sites, this observation suggests that these binding sites may differ in location within the membrane electric field.

An alternative explanation for the time-dependent change in voltage dependence of block is that glibenclamide interacts with a single binding site, whose position within the membrane field changes during a putative change in the conformation of the pore, induced by the voltage jump. However, this alternative scenario would require a voltage-induced conformational change in WT-CFTR, which has not been described, and would contradict the evidence for multiple binding sites obtained from steady-state single-channel studies where membrane potential is held constant (Zhang et al., 2004). Hence, we favor the hypothesis that glibenclamide interacts with at least two binding sites in the CFTR pore, and that these sites differ in on-rates and in voltage dependence. The overall voltage dependence of block and the macroscopic kinetics would then arise from contributions from both the fast on-rate and slow on-rate sites within the pore (as well as from a non-pore site that may contribute to steady-state inhibition of CFTR gating; Cui & McCarty, 2003).

Reconciling Microscopic and Macroscopic Kinetics

Based upon the observation that the site with slower on-rate, higher affinity, and greater voltage dependence makes a larger contribution to the fit of the time course of macroscopic blockade (Table 1), we propose that it is the slow on-rate site that has the larger impact on the voltage-dependent block of CFTR channels by glibenclamide, and has the higher affinity of the three sites within the pore due to a much slower off-rate. This is consistent with the designation of this site as contributing to the C3 state identified in single-channel experiments, which was characterized by higher affinity and greater voltage-dependence than the C2 state (Zhang et al., 2004). Furthermore, the single-channel summations confirm that time-independent and time-dependent interactions may be treated separately. In this regard, we propose that the rapid, time-independent block of macropatch currents at hyperpolarizing potentials reflects interactions with the sites that give rise to the C1 and C2 states, while the slow, time-dependent block reflects interactions with the site that gives rise to the C3 state (Fig. 12). Similarly, the rapid, time independent relief from block at depolarizing potentials reflects the dissociation of glibencla-

mide from the sites that give rise to the C1 and C2 states, while the slow, time-dependent relief from block reflects dissociation from the site that gives rise to the C3 state.

Blockade of CFTR currents by glibenclamide and by DPC is sensitive to mutations in the same region of the pore (McDonough et al., 1994; Gupta & Linsdell, 2002). Our single-channel experiments (Zhang et al., 2004) indicated that the concurrent presence of DPC and glibenclamide reduced the off-rate from the glibenclamide binding site that gives rise to the C3 state. Glibenclamide-mediated macroscopic current relaxations were also sensitive to the concurrent presence of DPC, which: 1) confirms that the slow macroscopic kinetics of block represent interactions between glibenclamide and the binding site giving rise to the C3 state; 2) suggests that the single binding site for DPC and the C3 binding site for glibenclamide may overlap; and 3) supports the notion that the inner vestibule of CFTR is large (Linsdell & Hanrahan, 1996; Zhou et al., 2002; Zhang et al., 2004). However, previous studies designed to determine the effects of pore-domain mutations on steady-state block of CFTR by glibenclamide, in order to identify the binding site(s), have not reported large changes in affinity for any single mutation (Gupta & Linsdell, 2002). This may be because no single-point mutation would be expected to destroy simultaneously all sites of interaction between the large drug molecule and the walls of the pore. Also, simply asking whether inhibition of steady-state current is affected by a given mutation does not identify which site was altered. In contrast, if initial block and time-dependent block represent interactions of glibenclamide with different sites in CFTR's pore, then we may be able to use these quantitative measures to separately assess the effects of mutations, in order to identify these sites.

Conclusions

In this study, we present evidence that glibenclamide blocks CFTR by a complex mechanism, including interactions with multiple binding sites that differ in voltage dependence and affinity, consistent with the model we proposed for steady-state inhibition of WT-CFTR single channels (Zhang et al., 2004). Glibenclamide blocks macroscopic currents in a time-dependent manner, with kinetics that reflect the microscopic kinetics of interactions of drug determined from single-channel experiments. These kinetics of macroscopic blockade may provide an added means of quantifying the effects of mutations and experimental conditions, in parallel with assessment of the efficacy of steady-state blockade. Hence, this study identifies quantitative assays that may be useful for further efforts to localize the glibenclamide binding sites in CFTR, in efforts to identify portions of the CFTR protein that line the pore.

This work was supported by the American Heart Association (9820032SE), the Cystic Fibrosis Foundation (MCCART00P0), and the NIH (DK056481). S. Zeltwanger was supported by an NIH postdoctoral training grant (DK07656). N.A.M. is an Established Investigator of the American Heart Association.

References

Al-Awqati, Q. 1995. Regulation of ion channels by ABC transporters that secrete ATP. *Science* **269:**805–806

Cai, Z., Lansdell, K.A., Sheppard, D.N. 1999. Inhibition of heterologously expressed cystic fibrosis transmembrane conductance regulator Cl^- channels by non-sulphonylurea hypoglycaemic agents. *Br. J. Pharmacol.* **128:**108–118

Cui, G., McCarty, N.A. 2003. Probing a new mechanism of glibenclamide interaction with CFTR: gating effects. *Biophys. J.* **84:**83a

Colquhoun, D., Hawkes, A.G. 1995. The principles of the stochastic interpretations of ion-channel mechanisms. *In:* Single-Channel Recording B. Sakmann, E. Neher, editors. pp. 397–482. Plenum Press, New York

Dawson, D.C. 1996. Permeability and conductance of ion channels: a primer. *In:* Molecular Biology of Membrane Transport Disorders, S.G. Shultz, editor. pp. 87–110. Plenum Press, New York

Dawson, D.C., Liu, X., Zhang, Z-R., McCarty, N.A. 2003. Anion conduction in CFTR: mechanisms and models. *In:* The CFTR Chloride Channel, K. Kirk, D,C. Dawson, editors. pp. 1–34. Landes Publishing, Georgetown, TX.

Goldstein, S.A.N., Miller, C. 1991. Site-specific mutations in a minimal voltage-dependent K^+ channel alter ion selectivity and open-channel block. *Neuron* **7:**403–408

Golstein, P.E., Boom, A., van Geffel, J., Jacobs, P., Masereel, B., Beauwens, R. 1999. P-glycoprotein inhibition by glibenclamide and related compounds. *Pfluegers. Arch.* **437:**652–660

Gupta, J., Linsdell, P. 2002. Point mutations in the pore region directly or indirectly affect glibenclamide block of the CFTR chloride channel. *Pfluegers. Arch.* **443:**739–747

Hanrahan, J.W., Tabcharani, J.A. 1990. Inhibition of an outwardly rectifying anion channel by HEPES and related buffers. *J. Membrane Biol* **116:**65–77

Haws, C., Krouse, M.E., Xia, Y., Gruenert, D.C., Wine, J.J. 1992. CFTR channels in immortalized human airway cells. *Am. J. Physiol.* **263:**L692–L707

Higgins, C.F., Linton, K.J. 2003. ABC transporters: An introduction and overview. *In:* ABC Proteins from Bacteria to Man, I.B. Holland, S.P.C. Cole, K. Kuchler, C.F. Higgins, editors. pp. xvii–xxiii. Academic Press, London, UK.

Ishihara, H., Welsh, M.J. 1997. Block by MOPS reveals a conformational change in the CFTR pore produced by ATP hydrolysis. *Am. J. Physiol.* **273:**C1278–C1289

Linsdell, P., Hanrahan, J.W. 1996. Disulphonic stilbene block of cystic fibrosis transmembrane conductance regulator Cl^- channels expressed in a mammalian cell line, and its regulation by a critical pore residue. *J. Physiol.* **496:**687–693

Mathews, C.J., Tabcharani, J.A., Chang, X.-B., Jensen, T.J., Riordan, J.R., Hanrahan, J.W. 1998. Dibasic protein kinase A sites regulate busting rate and nucleotide sensitivity of the cystic fibrosis transmembrane conductance regulator. *J. Physiol.* **508:**365–377

McCarty, N.A. 2000. Permeation through the CFTR chloride channel. *J. Exp. Biol.* **203:**1947–1962

McCarty, N.A., McDonough, S., Cohen, B.N., Riordan, J.R., Davidson, N., Lester, HA. 1993. Voltage-dependent block of the cystic fibrosis transmembrane conductance regulator Cl^- channel by two closely related arylaminobenzoates. *J. Gen. Physiol.* **102:**1–23

McDonough, S., Davidson, N., Lester, H.A., McCarty, N.A. 1994. Novel pore-lining residues in CFTR that govern permeation and open-channel block. *Neuron* **13:**623–634

Neher, E., Steinbach, J.H. 1978. Local anaesthetics transiently block currents through single acetylcholine-receptor channels. *J. Physiol.* **277:**153–176

Quick, M.W., Naeve, J., Davidson, N., Lester, H.A. 1992. Incubation with horse serum increases viability and decreases background neurotransmitter uptake in *Xenopus* oocytes. *BioTechniques* **13:**358–362

Riordan, J.R., Rommens, J.M., Kerem, B.-S., Alon, N., Rozmahel, R., Grzelczak, Z., Zielenski, J., Lok, S., Plavsic, N., Chou, J.-L., Drumm, M.L., lannuzzi, M.C., Collins, F.S., Tsui, L.-C. 1989. Identification of the cystic fibrosis gene: cloning and characterization of complementary DNA. *Science* **245:**1066–1072

Schultz, B.D., DeRoos, A.D.G., Venglarik, C.J., Singh, A.K., Frizzell, R.A., Bridges, RJ. 1996. Glibenclamide blockade of CFTR chloride channels. *Am. J. Physiol.* **271:**L192–L200

Sheppard, D.N., Robinson, K.A. 1997. Mechanism of glibenclamide inhibition of cystic fibrosis transmembrane conductance regulator Cl^- channels expressed in a murine cell line. *J. Physiol.* **503:**333–345

Walsh, K.B., Long, K.J., Shen, X. 1999. Structural and ionic determinants of 5-nitro-2-(3-phenylpropylamino)-benzoic acid block of the CFTR chloride channel. *Br. J. Pharmacol.* **127:**369–376

Winter, M.C., Sheppard, D.N., Carson, M.R., Welsh, M.J. 1994. Effect of ATP concentration on CFTR Cl^- channels: a kinetic analysis of channel regulation. *Biophys. J.* **66:**1398–1403

Zhang, Z.-R., McDonough, S.I., McCarty, N.A. 2000b. Interaction between permeation and gating in a putative pore domain mutant in the cystic fibrosis transmembrane conductance regulator. *Biophys. J.* **79:**298–313

Zhang, Z.-R., Zeltwanger, S., McCarty, N.A. 2000a. Direct comparison of NPPB and DPC as probes of CFTR expressed in *Xenopus* oocytes. *J. Membrane Biol.* **175:**35–52

Zhang, Z.-R., Zeltwanger, S., McCarty, N.A. 2004. Steady-state interactions of glibenclamide with CFTR: Evidence for multiple sites in the pore. *J. Membrane Biol.* **199:**15–28

Zhang, Z.-R., Zeltwanger, S., Smith, S.S., Dawson, D.C., McCarty, N.A. 2002. Voltage-sensitive gating induced by a mutation in the fifth transmembrane domain of CFTR. *Am.J.Physiol.* **282:**L135–L145

Zhou, Z., Hu, S., Hwang, T.-C. 2002. Probing an open CFTR pore with organic anion blockers. *J. Gen. Physiol.* **120:**647–662